ACS OMEGA

Open Access

http://pubs.acs.org/journal/acsodf

Article

Construction of a Novel Cuproptosis-Related ceRNA Network-SNHG3/miR-1306-5p/PDHA1 and Identification of SNHG3 as a Prognostic Biomarker in Hepatocellular Carcinoma

Yong Pan, Yiru Zhang, Xiaodan Hu, and Shibo Li*

Cite This: *ACS Omega* 2023, 8, 38690−38703

Read Online

ACCESS | Metrics & More | Article Recommendations | Supporting Information

ABSTRACT: The crucial role of competitive endogenous RNA (ceRNA) in the malignant biological behavior of tumors has been certificated. Nevertheless, the detailed function and molecular mechanism of ceRNA associated with cuproptosis in hepatocellular carcinoma (HCC) remains dismal. In this study, we first constructed a protein−protein interaction network and identified the module with the highest degree of aggregation degree. DLAT and PDHA1 were screened out of the module after differential expression and survival analysis. Next, we reverse-predicted the upstream miRNA and lncRNA from mRNA (DLAT, PDHA1) and successfully established the ceRNA network-SNHG3/miR-1306-5p/PDHA1. SNHG3 was identified to be an independent prognostic biomarker based on the outcome of univariate and multivariate Cox analyses. Subsequently, we implemented methylation, immune infiltration, and drug sensitivity analysis to investigate the potential biological functions of SNHG3 in HCC. In addition, SNHG3 expression was upregulated in liver cancer cell lines. In vitro functional assay revealed that SNHG3 knockdown significantly attenuated proliferation, migration, and invasion of liver cancer cells. In summary, SNHG3 exhibited oncogenic characterization via sponging miR-1306-5p to regulate PDHA1, which might function as a promising prognostic indicator and a potential therapeutic target for HCC and shed new light on the molecular mechanism of HCC progression.

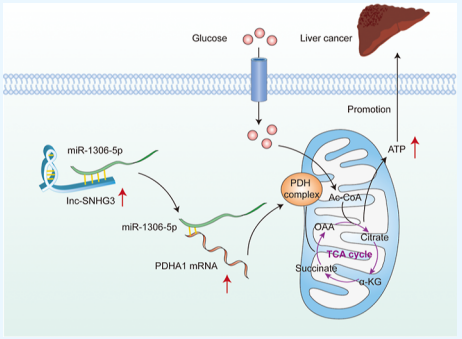

1. INTRODUCTION

Liver cancer is the third leading cause of cancer-related fatalities globally, posing a severe threat to human health and life.[1] Hepatocellular carcinoma (HCC) is the most common subtype of liver cancer, taking up 85−90% of all primary liver cancers.[2,3] Although significant advances have been made in risk factors,[4] early diagnosis,[5] surveillance methods,[6] and treatment techniques for HCC,[7] due to its insidious onset, rapid growth, high malignancy, and susceptibility to invasive metastasis, more than 70% of patients diagnosed with HCC are already deprived of the chance of surgery or liver transplantation, resulting in an extremely poor prognosis.[8] Therefore, predicting the prognosis of HCC patients is of great significance in guiding individualized treatment, prolonging the overall survival of patients, and improving long-term treatment outcomes. The predictive tools that have been developed for clinical use include serological biomarkers[9,10] and various staging systems.[11] Although these predictive tools have proven to be of some use, their predictive efficiency remains limited, as they do not address the biological features of HCC and the genetic and epigenetic alterations of the tumor.

Long noncoding RNAs (lncRNAs) are a series of RNA molecules with transcripts larger than 200 nucleotides and without protein translation functions. However, they can regulate the expression of target genes at multiple levels and thus participate in a range of crucial biological processes.[12−14] Salmena et al. proposed that noncoding RNA including lncRNA, mRNA, and circRNA could produce a modulatory effect of ceRNA by competing with the same miRNA response elements.[12] In recent years, several studies have confirmed the role of ceRNA regulatory networks in the development of HCC. For instance, Li et al. proposed that the TRHDE-AS1/PKIA ceRNA network may elucidate the mechanism by which TPX2 improved the prognosis of HBV-related HCC.[15] Hao et al. uncovered that pseudogene UBE2MP1-derived transcript acted as a molecular sponge for miR-145-5p to enhance cell growth and apoptosis resistance of HCC cells in vitro.[16] Although there was growing evidence that dysregulated lncRNAs were correlated with tumorigenesis, metastasis, and prognosis in HCC, few studies have explored the mechanisms of lncRNA regulation and used them for prognostic prediction in HCC.

Received: August 15, 2023
Accepted: September 22, 2023
Published: October 3, 2023

In 2022, Tsvetkov et al. systematically reported a mitochondrial respiration-dependent, proteolipidylation-mediated cell death for the first time that was distinct from "apoptosis,"[17] "necroptosis,"[18] "pyroptosis,"[19] "ferroptosis,"[20] and named it after "cuproptosis" (copper-induced cell death).[21] Extensive research has shown that copper is tightly linked to the metabolism and metastasis of cancer by influencing the respiratory function of mitochondria and the process of glycolysis, insulin resistance, and lipid metabolism.[22−24] Moreover, several previous studies have mentioned that copper plays vital parts in the initiation and progression of HCC. Jin et al. recognized a new copper complex that could inhibit methionine cycle metabolism in HCC.[25] Copper metabolism gene MURR1 domain 10 (COMMD10), a crucial gene engaging in copper metabolism, has been reported to prevent proliferation and facilitate apoptosis by inhibiting NF-κB signaling in HCC.[26] Researchers also found that COMMD10 inhibited HIF1α/CP loop by disrupting Cu−Fe balance in HCC, thus revealing a novel role for copper in promoting the radio resistance of HCCs.[27] However, the association between cuproptosis and the prognosis of HCC is still undetermined.

Our study established a cuproptosis-related ceRNA network—SNHG3/miR-1306-5p/PDHA1 in HCC using bioinformatics tools (Figure 1). Next, we identified SNHG3 as an independent prognostic indicator and analyzed its correlation with methylation, immune infiltration, and drug sensitivity in HCC. Finally, we verified SNHG3 overexpression in liver cancer cell lines compared with normal hepatocytes using qRT-PCR and demonstrated that SNHG3 contributed to the proliferation, migration, and invasion of HCC in vitro experiments. Hopefully, our research will provide a useful prognostic indicator and a potential therapeutic target for HCC and contribute to elucidating the molecular mechanism of tumorigenesis in HCC.

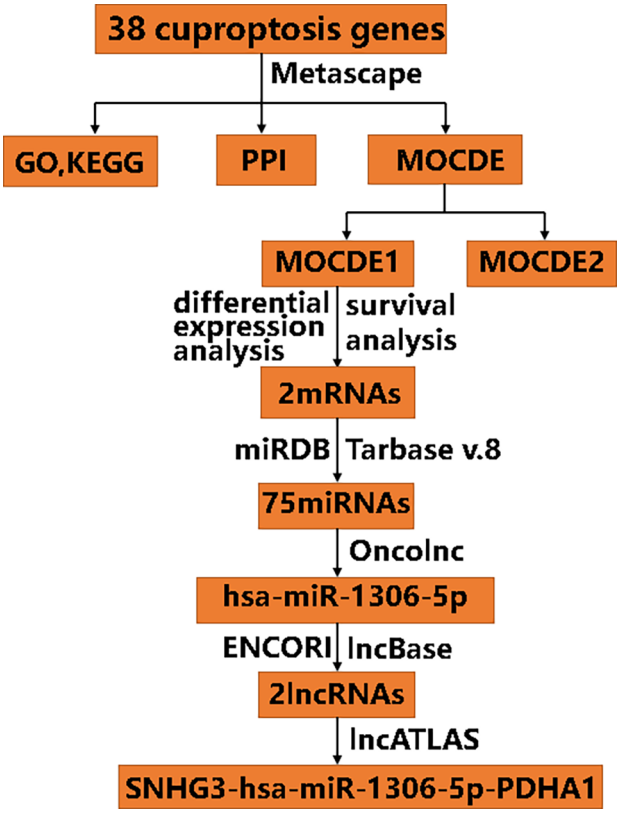

Figure 1. Flowchart of construction of the cuproptosis-related ceRNA network.

2. MATERIALS AND METHODS

2.1. HCC-Related Data Acquisition. The Cancer Genome Atlas (TCGA, http://portal.gdc.com/) database is an important bioinformatic tool and service resource for research. Gene expression profiling microarrays for HCC were obtained from TCGA, containing 374 HCC tissue samples and 50 adjacent nontumorous tissue samples. Additionally, six data sets (GSE136247, GSE45436, GSE55092, GSE45267, GSE36376, and GSE14520) were collected for validation from the gene expression omnibus (GEO) database (http://www.ncbi.nlm.nih.gov/geo/). The clinical information on patients in the TCGA cohort is illustrated in Table S1. Given that the data above were all publicly available online, there is no need for an ethical review.

2.2. Functional Enrichment and Protein−Protein Interaction Analysis. According to preceding research,[21,23,28] 38 cuproptosis-related genes were determined. The full name and function of 38 cuproptosis-correlated genes are listed in Table S2.

To understand the potential molecular function of these genes, Gene Ontology (GO) and Kyoto Encyclopedia of Genes and Genomes (KEGG) analysis was performed using the online tool Metascape (http://metascape.org).[29] The protein−protein interaction network and MCODE algorithm[30] were also carried out to find highly aggregated proteins with similar functions by Metascape.

2.3. Differential Expression and Survival Analysis. To further explore the role of MCODE1 genes in HCC, differential expression analysis was conducted between HCC and normal tissues. The overall survival (OS) analysis was carried out using the "survival" R package. The hazard ratio was calculated using Cox proportional hazards model and Kaplan−Meier model, with the median set as the cutoff value. Then, DLAT and PDHA1 were selected because of their prognostic value in HCC, and their differential expression was validated by Human Protein Atlas (HPA, https://www.proteinatlas.org/) database.

2.4. Construction and Validation of ceRNA Network. According to the concept and mechanism of ceRNA hypothesis, it has the following characteristics: (a) identical miRNA binding sites for ceRNAs, (b) ceRNA are all regulated by miRNAs, (c) there is a reciprocal regulatory relationship between ceRNAs and a consistent trend in expression levels, and (d) lncRNAs play a predominantly endogenous competitive role in the cytoplasm. Therefore, the ceRNA network was built following the steps below: (1) miRDB and Tarbase v.8 were utilized to find out the miRNAs targeting mRNA; (2) mRNA-miRNA regulatory network was visualized by Cytoscape software;[31] (3) Oncolnc (http://www.oncolnc.org/) was utilized to perform survival analysis on miRNAs; (4) Screened out miRNA was put into both miRDB (http://www.mirdb.org/) and lncBasev.3 (https://diana.ece.uth.gr/lncbasesv3/); (5) the "VennDiagram" R package was utilized to select out lncRNAs targeting miRNA shared by both miRDB and lncBasev.3; (6) lncATLAS (https://lncatlas.crg.eu)[32] was used to filter out nuclear lncRNAs; and (7) the ceRNA network-SNHG3/miR-1603-5p/PDHA1 was eventually constructed.

https://doi.org/10.1021/acsomega.3c06018
ACS Omega 2023, 8, 38690−38703

After the process of establishing ceRNA network, TargetScan (http://www.targetscan.org/) database was utilized to forecast binding domain of lncRNA-miRNA and mRNA-miRNA in the ceRNA network. In addition, the abnormal expression of lncRNA and mRNA in the ceRNA network was demonstrated by CCLE (https://sites.broadinstitute.org/ccle/) database and ICGC database.

2.5. Differential Expression Validation of SNHG3 and PDHA1. For validation, six independent data sets (GSE136247, GSE45436, GSE55092, GSE45267, GSE36376, and GSE14520) were collected, and their information, including platform, sample type, and source type, is summarized in Table S3. The column bar graph was drawn to represent the differential expression of SNHG3 and PDHA1 in various data sets by GraphPad Prism v9.3.1.

To increase the statistical reliability of this study, a meta-analysis of differential expression results of various data sets was implemented by inputting mean and standard deviation. Heterogeneity between different data was measured by the Q test (I2 statistics). Besides, a forest plot was drawn to present the mean difference and correlated 95% CI of SNHG3 and PDHA1. All steps were completed with the software Review Manager5.4.

2.6. Independent Prognostic Analysis and Construction of Nomogram. Univariate Cox analysis was used to evaluate the relationship between the OS and characteristics (SNHG3 expression, PDHA1 expression, and various clinical factors). Multivariate Cox analysis was used to recognize independent prognostic factors in HCC patients. A nomogram was constructed to integrate all predictive characteristics in the multivariate Cox regression model using "rms" package. Besides, the calibration curve was created to assess the model's predictive capacity.

2.7. Methylation, Immune Infiltration, and Drug Sensitivity Analysis. The correlation between methylation and expression of SNHG3 in HCC patients was investigated using the GSCALite database (http://bioinfo.life.hust.edu.cn/web/GSCALite/).[33] Then, the methylation degree of SNHG3 was evaluated by UALCAN (http://ualcan.path.uab.edu/) and DiseaseMeth version 2.0 (http://bio-bigdata.hrbmu.edu.cn/diseasemeth/). Besides, the methylation site of SNHG3 DNA sequence correlation with gene expression was visualized through MEXPRESS (https://mexpress.be/).

The TIMER2.0 database (https://cistrome.shinyapps.io/timer/)[34] was utilized to explore the association between SNHG3 expression and immune cell infiltration and provide the comparison of tumor infiltration levels in HCC with different somatic copy number alterations for SNHG3. TIMER2.0 database utilizes the "immunedeconv,"[35] an R package which integrates six state-of-the-art algorithms to make reliable immune infiltration estimations. Since the expression of immune checkpoint-related genes was associated with the immunotherapy effect,[36] we further evaluated the connection between three vital immune checkpoints (ICKs), including PDCD1, CD274, and HAVCR2 in HCC using Spearman correlation analysis.

In addition, the CTRP database (http://portals.broadinstitute.org/ctrp/) was applied to detect the correlation between SNHG3 expression and sensitivity of small-molecule drugs.

2.8. Cell Culture and Transfection. The liver cancer cell lines (HepG2, Bel7402, HCCLM3, and MHCC97H) and normal liver cells (L02) are given by Dr Haijie Ma. All cells were placed in a thermostat incubator with the condition of 37 °C, 5% CO_2. L02 cells were cultured using the RPMI1640 medium supplemented with 10% fetal bovine serum (FBS), while HepG2, Bel7402, HCCLM3, and MHCC97H cells were nurtured by Dulbecco's modified Eagle's medium (DMEM) high-glucose medium combining with 10% FBS. We used Lipofectamine 3000 Transfection Reagent (Invitrogen, USA) and short-interfering RNA targeting SNHG3 (si-SNHG3-1, 5′-GGGCACUUCGUAAGGUUUA-3′; si-SNHG3-2, 5′-GACCAAUAGGACCGUAAGU-3′) and their negative control (si-NC, 5′-TTCTCCGAACGTGTCACGT-3′) (Zixi Biotechnology Co. Ltd., China) to make transfection in Bel7402 and HCCLM3 cells. Bel7402 and HCCLM3 cells were evenly plated in 6-well plates. Twenty-four hours before transfection, $2-6 \times 10^5$ cells were incubated in 1500 μL of medium with 60−80% confluence for transfection. Twenty-four hours after transfection, qRT-PCR was utilized to examine cell transfection efficiency.

2.9. Quantitative Real-Time PCR. RNA was extracted from L02, HepG2, HCCLM3, Bel7402, and MHCC97H cells using TRIzol reagent, followed by reverse-transcription to synthesize cDNA using a RT reagent Kit (Perfect Real Time). According to the SYBR-Green method (TaKaRa), the thermal cycler Real-time System was applied to detect quantitative PCR from the $2^{-\Delta\Delta Cq}$ methods. The primers are listed as follows: SNHG3: Forward 5′-TTCAAGCGATTCTCGTGCC-3′, Reverse 5′-AAGATTGTCAAACCCT.

CCCTGT-3′. GAPDH: Forward 5′-TCAAGATCATCAGCAATGCC-3′, Reverse 5′-CGATACCAAAGTTGTCATGGA-3′.

2.10. Cell Proliferation Assay. Cell proliferation was measured by a CCK8 kit (BOSTON, USA). Each well in 96-well plates was planted with 4×10^3 cells. Ten microliters of CCK-8 reagent was put into each well at 0, 24, 48, and 72 h after transfection, and the cells were incubated at 37 °C for 2 h without light. Then, the absorbance was read at 450 nm on the enzyme labeling instrument.

2.11. Wound Healing Assay. When transfected cells reached about 90% confluence in 6-well plate, we scratched vertically with sterile 200 μL pipet tip compared to the ruler and then substituted the old medium with serum-free medium. After 24 h, the cell migration status was observed and photographed. Besides, the images were analyzed by ImageJ.

2.12. Transwell Assay. The invasion was identified by transwell assay. Eighty microliters of Matrigel matrix (corning, American) diluted by DMEM high-glucose medium at 1:20 was added to the surface of the transwell chambers and placed in 37 °C incubator for solidification about 2 h. The transfected cells were planted in transwell chambers and incubated for 24 h. The upper chamber was filled with 200 μL of cell suspension (1×10^6/mL), while the lower chamber was added with a complete medium with 10%FBS. Subsequently, unmigrated cells in the upper chamber were wiped off gently, and the invaded cells in the lower chamber were fixed by methanol and stained with 0.1% crystal violet. Finally, photos were taken with a microscope.

2.13. Statistical Analysis. As for the statistical description, numerical variables were measured as mean ± standard deviation, while categorical parameters were evaluated as frequency and proportion. The student's *t*-test and Mann−Whitney *U* test were utilized to compare the difference between two data groups.

https://doi.org/10.1021/acsomega.3c06018
ACS Omega 2023, 8, 38690−38703

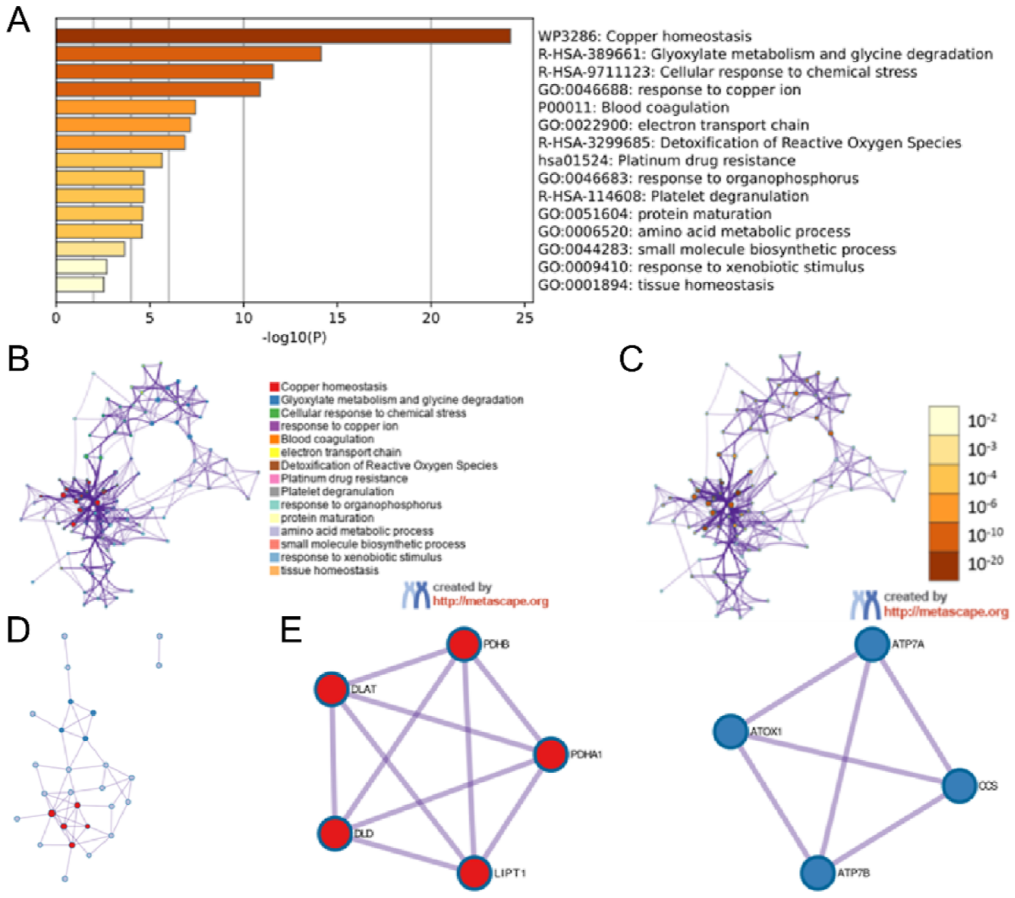

Figure 2. Functional enrichment and protein−protein interaction analysis of cuproptosis-related genes. (A) Bar graph of enriched terms across input gene lists, colored by *p*-values. (B) Network of enriched terms: colored by cluster ID, where nodes that share the same cluster ID are typically close to each other. (C) Network of enriched terms: colored by *p*-value, where terms containing more genes tend to have a more significant *p*-value. (D) Protein−protein interaction network. (E) Two identified densely connected network components by using the MOCDE algorithm.

All the analysis methods and R package were conducted by R (3.6.3) software. A difference of $P < 0.05$ was considered statistically significant ($^{*}p < 0.05$; $^{**}p < 0.01$; $^{***}p < 0.001$), and all P values were two-tailed.

3. RESULTS

3.1. Functional Enrichment Analysis and Protein−Protein Interaction Network of Cuproptosis-Related Genes. Using the Metascape online database, the functional enrichment analysis of 38 cuproptosis-related genes was implemented with different ontology sources such as KEGG Pathway, GO Biological Processes, and Reactome Gene Sets. As shown in Figure 2A, the main enriched terms were "Copper homeostasis," "Glyoxylate metabolism and glycine degradation," "Cellular response to chemical stress," and "response to copper ion." To further explore the internal connection between the terms, a subgroup of enriched terms has been chosen and presented as a network plot (Figure 2B,C). Moreover, a PPI network consisting of 28 nodes and 46 edges was constructed and visualized (Figure 2D). In addition, we identified 2 significant clusters by using the MCODE algorithm (Figure 2E), and the biological functions of each cluster were interpreted. The genes in clustering MOCDE1 were primarily associated with glyoxylate metabolism and glycine degradation, the acetyl-CoA biosynthetic process from pyruvate, and the acetyl-CoA biosynthetic process. The genes in clustering MOCDE2 were mainly correlated with copper homeostasis, cellular copper ion homeostasis, and copper ion transport.

3.2. Expression Landscape and Prognostic Value of DLAT, DLD, LIPT1, PDHA1, and PDHB in HCC. Given that clustering MOCDE1 was most tightly connected, we chose the genes in MOCDE1 (DLAT, DLD, LIPT1, PDHA1, and PDHB) for the following step analysis. To evaluate the role of these genes in the initiation and progression of HCC, we implemented differential expression analysis between HCC tissues and normal liver tissues and survival analysis in HCC samples. Differential expression analysis revealed that the expression of 5 cuproptosis-related genes was upregulated in HCC samples (Figure 3A−E). Survival analysis showed that only DLAT and PDHA1 could significantly affect the OS rate of HCC patients using the Cox proportional hazards model and the Kaplan−Meier model (Figure 3F−J). Interestingly, high expression of DLAT and PDHA1 was both significantly linked to poor OS in HCC patients. Furthermore, we validated the differential expression of DLAT and PDHA1 at the translational level through the HPA database (Figure 3K,L).

3.3. Construction of a Triple Regulatory Network of mRNA-miRNA-lncRNA. According to the ceRNA hypothesis, we reverse-predicted the miRNAs targeting two mRNAs (DLAT, PDHA1) with prognostic values. The results showed that a total of 75 miRNAs were found by the miRDB and Tarbase v.8 databases. We visualized the mRNA-miRNA regulatory network using Cytoscape software (Figure 4A).

https://doi.org/10.1021/acsomega.3c06018
ACS Omega 2023, 8, 38690−38703

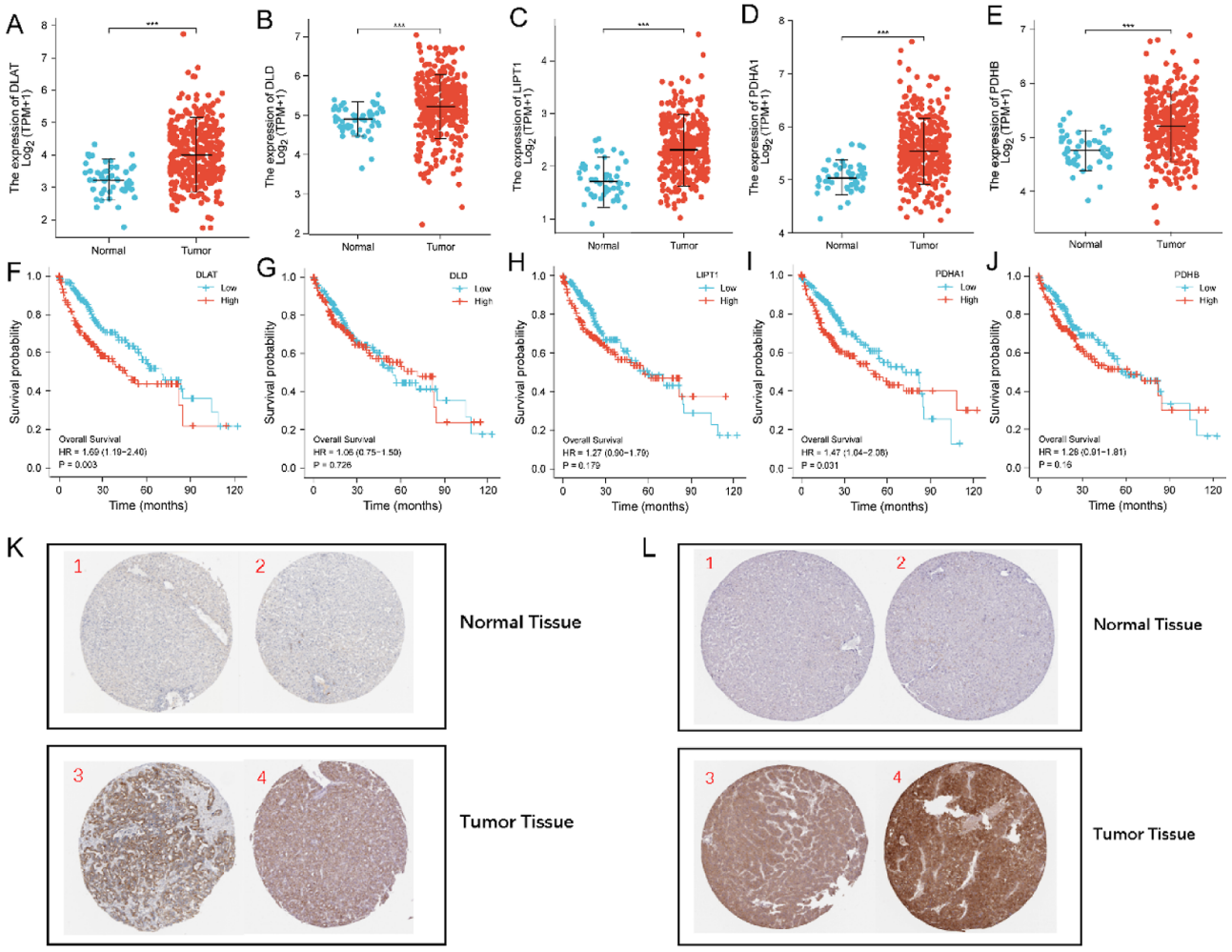

Figure 3. Expression landscape and prognostic value of 5 cuproptosis-related genes in HCC. (A−E) Differential expression analysis of DLAT (A), DLD (B), LIPT1 (C), PDHA1 (D), and PDHB (E) between HCC samples and normal samples in TCGA. (F−J) Survival analysis of DLAT (F), DLD (G), LIPT1 (H), PDHA1 (I), and PDHB (J) in HCC samples in TCGA. (K,L) Validation of the expression of DLAT (K), PDHA1 (L) on the translational level by the Human Protein Atlas database (immunohistochemistry).

Next, we put 75 miRNAs into the Oncolnc database and identified one miRNA, miR-1306-5p, whose expression was negatively linked to OS of HCC patients both in single-factor Cox regression analysis (Cox Coefficient = 0.3, $P = 2.00 \times 10^{-3}$) and log-rank test ($P = 0.008$). Moreover, we screened two lncRNAs (SNHG3, MALAT1) targeting miRNA shared by both miRDB and the lncBasev.3 database (Figure 4B). We discovered that only SNHG3 was located in the cytoplasm by using the lncATLAS database (Figure 4C). Thus, a ceRNA network- SHNG3/miR-1306-5p/PDHA1 was established. To verify the regulatory role of the ceRNA network in HCC, we performed differential expression and survival analysis of lncRNA (SNHG3) and mRNA (PDHA1). The results showed that the SNHG3 expression was significantly upregulated in HCC (Figure 4D) and that SNHG3 overexpression was linked to poor OS of HCC patients (Figure 4E). We also demonstrated the positive correlation between SNHG3 and PDHA1 in HCC (Figure 4F). Finally, the binding sites in the SNHG3 and PDHA1 3′UTRs were predicted to match miR-1306-5p by ENCORI (Figure 4G) and TargetScan (Figure 4H), respectively.

3.4. External Validation of SNHG3 and PDHA1 Abnormally High Expression. To verify SNHG3 and PDHA1 abnormally high expression in HCC, we conducted differential expression analysis in six GEO data sets (GSE136247, GSE45436, GSE55092, GSE45267, GSE36376, and GSE14520). The results revealed that both SNHG3 (GSE136247: $t = 3.577$, $p = 0.0007$; GSE45436: $t = 3.310$, $p = 0.0012$; GSE55092: $t = 3.793$, $p = 0.0002$; Figure 5A−C) and PDHA1 (GSE45267: $t = 2.532$, $p = 0.0132$; GSE36376: $t = 11.62$, $p < 0.0001$; GSE14520: $t = 2.550$, $p = 0.0111$; Figure 5E−G) exhibited a remarkable overexpression trend in most HCC tumors. Given the heterogeneity between different data sets (including the TCGA-LIHC cohort), we employed the random effects model for the meta-analysis. We uncovered that both SNHG3 (Figure 5D) and PDHA1 (Figure 5H) were still significantly overexpressed in HCC tumor tissues compared with nontumor tissues after combing all the study outcomes.

3.5. Screening Independent Prognostic Factor of SNHG3/hsa-miR-1306-5p/PDHA1 in HCC Patients. To identify independent prognostic factors, SNHG3 expression, PDHA1 expression, and clinical characteristics were subjected to univariate and multivariate Cox analyses.

In univariate Cox regression analysis (Figure 6A), tumor diameter, distant metastasis, SNHG3 expression, and PDHA1 expression were tightly connected to the poor OS of HCC

https://doi.org/10.1021/acsomega.3c06018
ACS Omega 2023, 8, 38690−38703

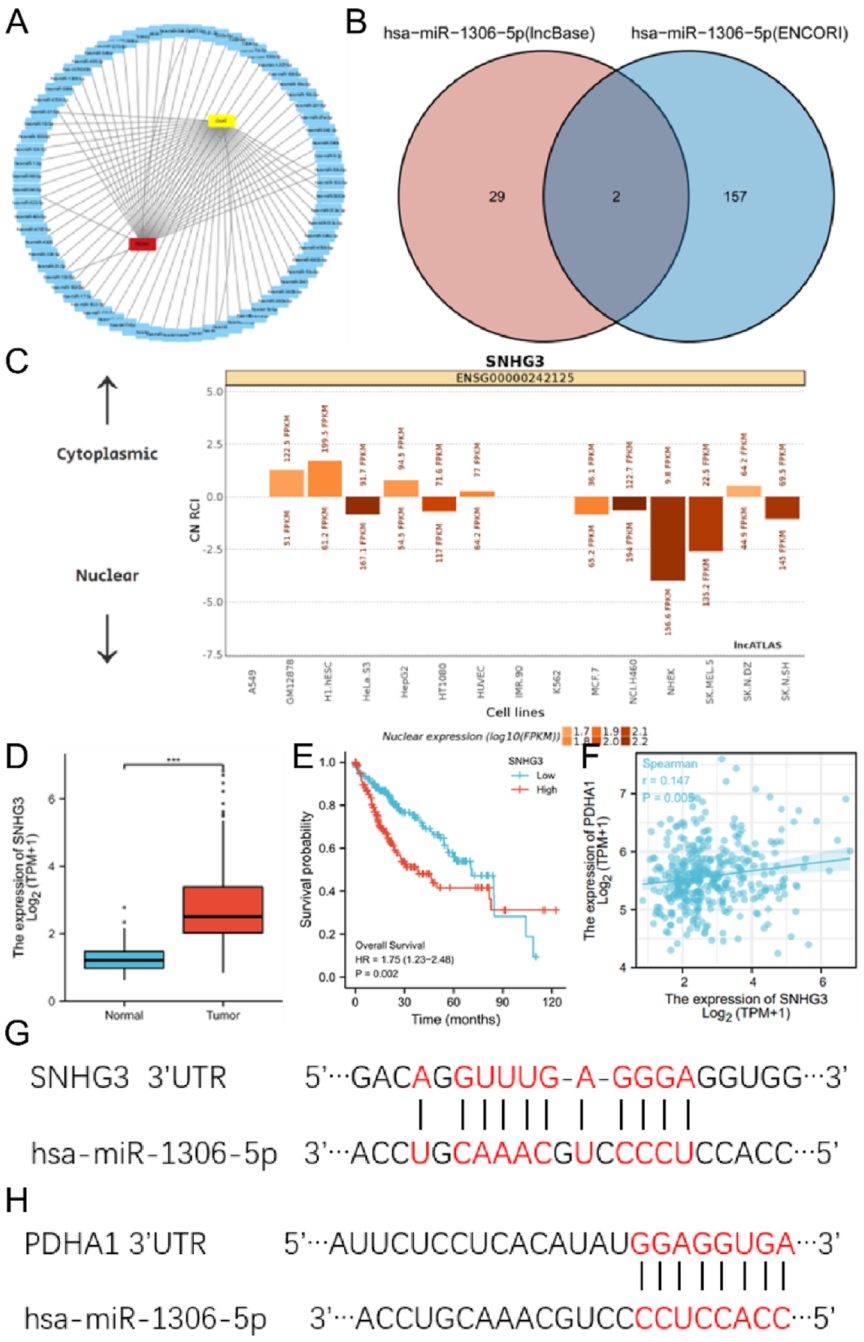

Figure 4. Construction of the mRNA-miRNA-lncRNA triple regulatory network. (A) The lncRNA-miRNA-mRNA triple regulatory network in HCC. Red indicates upregulated. (B) Results of miRNA reverse prediction lncRNA. (C) Cytoplasmic/nuclear localization of SNHG3: RCI and expression values (all cell types). (D) Expression of SNHG3 was significantly upregulated in HCC. (E) Kaplan−Meier curves of SNHG3 in patients with HCC in the low and high expression groups. (F) Correlation analysis between SNHG3 and PDHA1 in HCC. (G) Binding sites between SNHG3 and hsa-miR-1306-5p predicted by the ENCORI database. (H) Binding sites between PDHA1 and hsa-miR-1306-5p predicted by the TargetScan database.

patients. In multivariate Cox regression analysis (Figure 6B), only tumor diameter and SNHG3 expression were still linked to the OS in HCC patients. All factors in the multivariate Cox regression model were included to establish a nomogram (Figure 6C). The calibration curve (Figure 6D) showed that the nomogram had an excellent predictive capacity. Besides, the hazard proportional curve (Figure 6E) exhibited Cox regression coefficients for SNHG3 at different prognosis times.

Therefore, our results suggested that SNHG3 may become an independent prognostic factor for HCC patients.

3.6. Indicative Role of SNHG3 Expression in Methylation, Immune Infiltration, and Drug Sensitivity of HCC.

Given that SNHG3 was more likely to become an independent factor, we further analyzed SNHG3 in detail. To clarify the mechanism of SNHG3 anomalous upregulation in HCC tissues, we explored the association between SNHG3 expression and its methylation conditions using different methods. Figure 7A shows that gene expression and methylation levels of SNHG3 are most closely associated among all hub genes in HCC. We also found that the

https://doi.org/10.1021/acsomega.3c06018
ACS Omega 2023, 8, 38690−38703

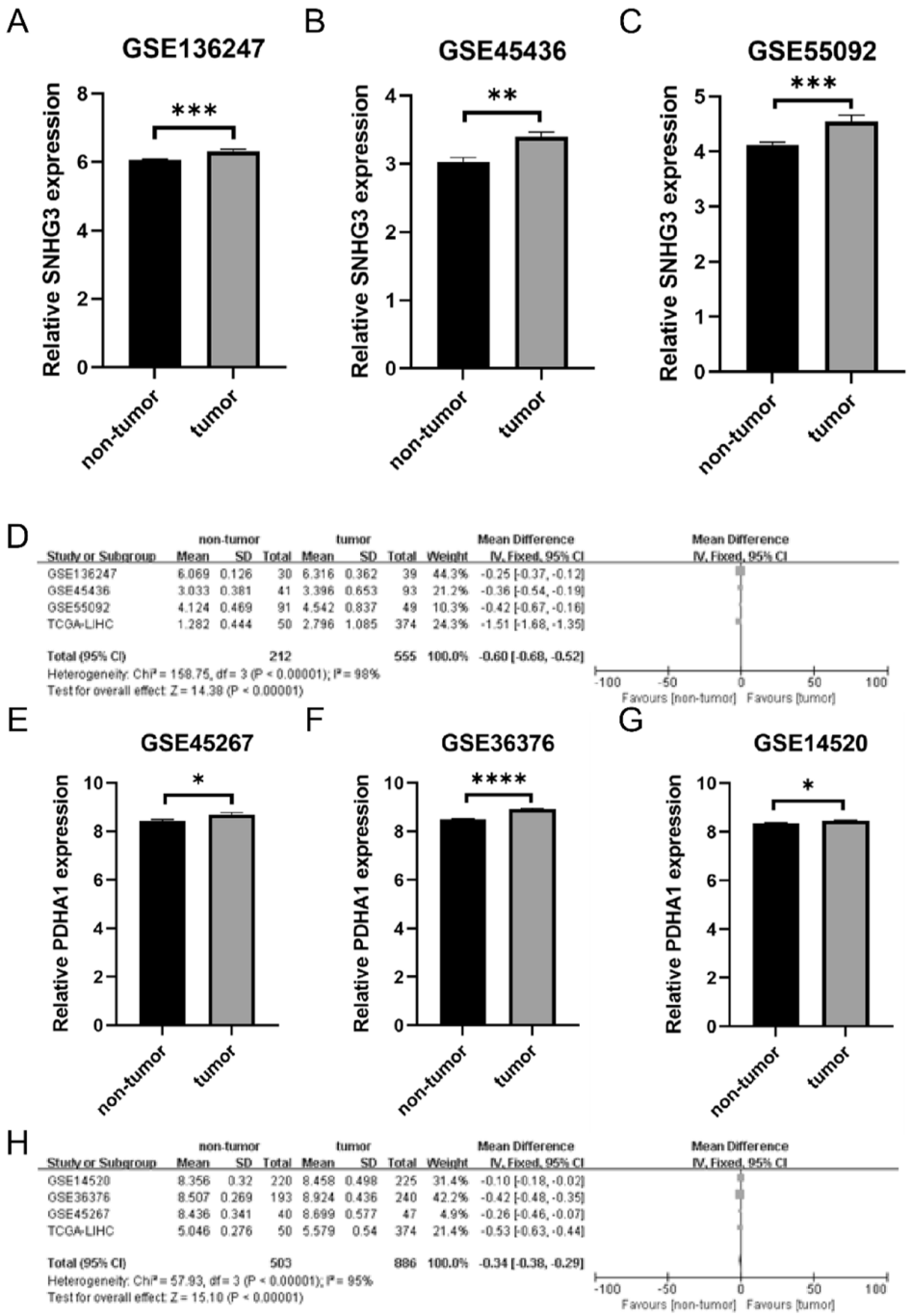

Figure 5. External validation of SNHG3 and PDHA1 abnormally high expression. Differential expression levels of SNHG3 with HCC in GSE136247 (A), GSE45436 (B), GSE55092 (C), and corresponding meta-analysis outcome (D). Differential expression levels of PDHA1 with HCC in GSE45267 (E), GSE36376 (F), and GSE14520 (G) and corresponding meta-analysis outcome (H).

methylation level of SNHG3 in normal samples was higher compared with HCC tumor samples in both the UALCAN database (Figure 7B) and the DiseaseMeth database (Figure 7C). Furthermore, we detected 10 methylation sites (cg25775721, cg24469114, cg26419621, cg15161854, and cg07807470) in the DNA sequences of SNHG3 that had a negative correlation with their expression at a standard of *P* value <0.001 (Figure 7D).

We also assessed the correlation between SNHG3 expression and immune infiltration in HCC using the TMMIR database, since immune cells in the tumor microenvironment affected the prognosis of various cancers. As shown in Figure 8A, infiltration abundance of neutrophils was possibly associated with SNHG3 gene copy number. We discovered that SNHG3 expression was positively linked to tumor purity and infiltration abundance of B-cells, $CD4^+$ T-cells, $CD8^+$ T-cells, macrophages, neutrophils, and dendritic cells (Figure 8B). To identify whether SNHG3 expression could potentially influence immunotherapy efficacy, we investigated the association between SNHG3 expression and three vital immune checkpoints (PDCD1, HAVCR2, and CD274) expression. Figure 8C−E shows that SNHG3 expression was positively correlated with PDCD1 expression

https://doi.org/10.1021/acsomega.3c06018
ACS Omega 2023, 8, 38690−38703

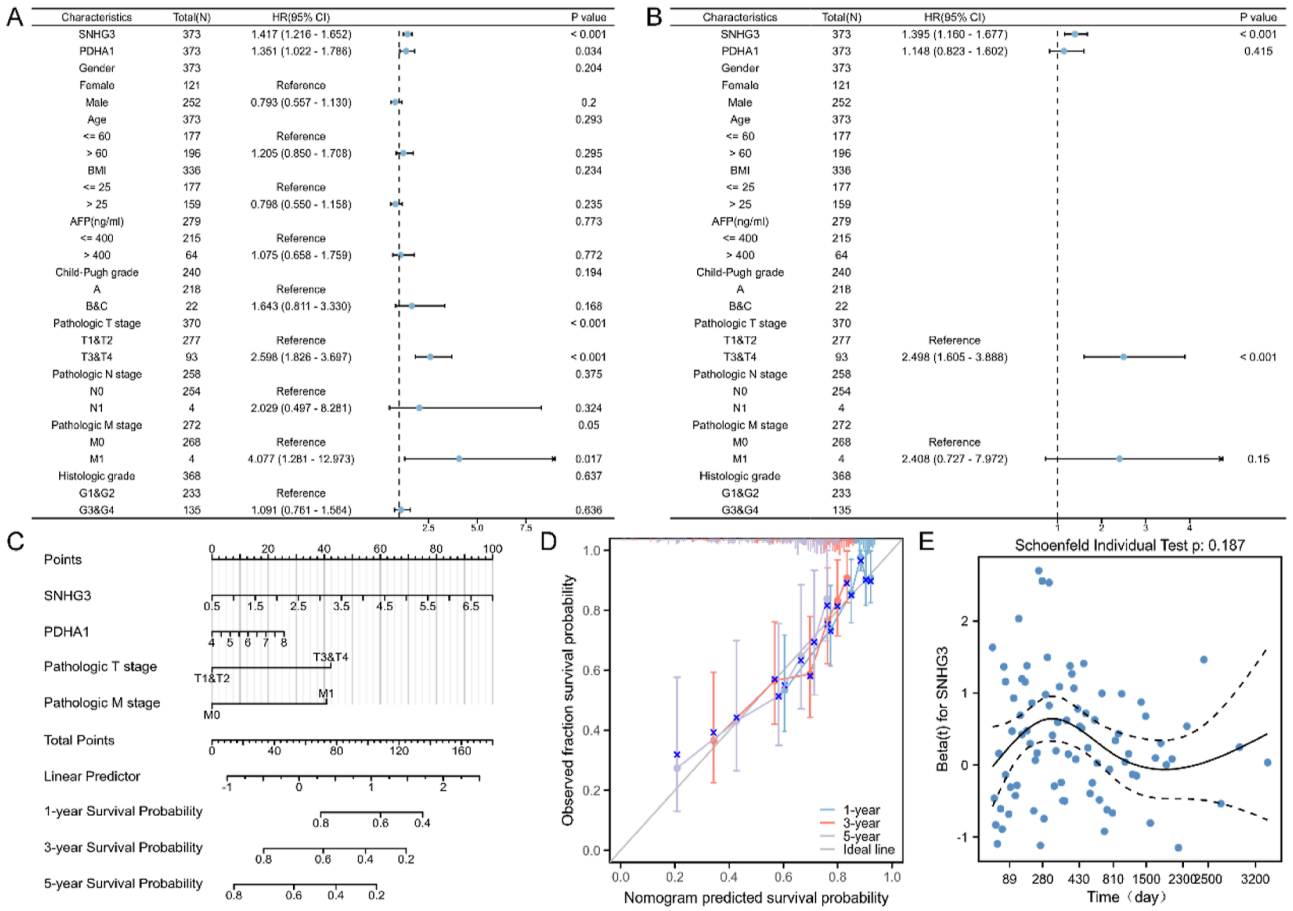

Figure 6. Independent prognostic factor screening and nomogram construction. Univariate Cox analysis (A) and multivariate Cox analysis (B) of clinical characteristics, SHNG3 expression, and PDHA1 expression. (C) Construction of the nomogram model. (D) Calibration curve of the nomogram. (E) Hazard proportional curve of SNHG3.

and HAVCR2 expression, while SNHG3 expression had no notable association with CD274.

In addition, we found that SNHG3 expression was positively correlated with drug sensitivity of BRD-K44224150 (Figure 8F), fulvestrant (Figure 8G), darinaparsin (Figure 8H), and tubastain A (Figure 8I).

3.7. lncRNA SNHG3 Is Overexpressed in Liver Cancer Cell Lines. We considered a few liver cancer cell lines (HepG2, Bel7402, HCCLM3, and MHCC97H) as the experimental group, with normal hepatocyte (L02) as the control group, and the result suggested that SNHG3 was overexpressed in liver cancer cell lines (Figure 9A). Given that Bel7402 and HCCLM3 cell lines exhibited the top two highest SNHG3 expression, we chose them for subsequent experimental validation in vitro. The qRT-PCR was utilized to examine the knockdown efficiency. The bar graphs indicated that the transfection made by short-interfering RNA targeting SNHG3 (si-SNHG3-1 and si-SNHG3-2) and their negative control (si-NC) was relatively successful in Bel7402 (Figure 9B) and HCCLM3 (Figure 9C) cell lines.

3.8. The lncRNA SNHG3 Knockdown Inhibits HCC Cell Proliferation, Migration, and Invasion. To explore the molecular biological functions of lncRNA SNHG3 in modulating cancer cell phenotypes, we performed functional interference in HCC cells. The results of CCK-8 assay suggested that SNHG3 interference could significantly inhibit the proliferation activity of Bel7402 and HCCLM3 cell lines (Figure 9D,E). The data from wound healing (Figure 9F,G) and transwell assay (Figure 9H,I) suggested that lncRNA SNHG3 silence could remarkably attenuate migration and invasion abilities of Bel7042 and HCCLM3 cell lines. These findings demonstrated that lncRNA SNHG3 could promote the progression of HCC.

4. DISCUSSION

HCC is one of the most common malignancies worldwide, and its development is a complex biological process with multigene involvement, multifactorial effects, and multistage progression. Although significant progress has been made in the diagnosis and treatment of HCC, the potential molecular mechanism of HCC still needs to be fully illuminated and requires investigation to further improve the prognosis of patients with HCC. This study identified a cuproptosis-related ceRNA regulatory network which probably contributed to explaining the molecular mechanism of HCC carcinogenesis and provided a promising prognostic biomarker and a therapeutic target for HCC patients.

Cuproptosis, a new type of cell death, has attracted more and more attention. The results of functional enrichment showed that cuproptosis-related genes were jointly involved in the processes of copper homeostasis, glyoxylate metabolism, glycine degradation, cellular response to chemical stress, and blood coagulation. Wu et al. reported that an imbalance of copper homeostasis could lead to detrimental outcomes to the

https://doi.org/10.1021/acsomega.3c06018
ACS Omega 2023, 8, 38690−38703

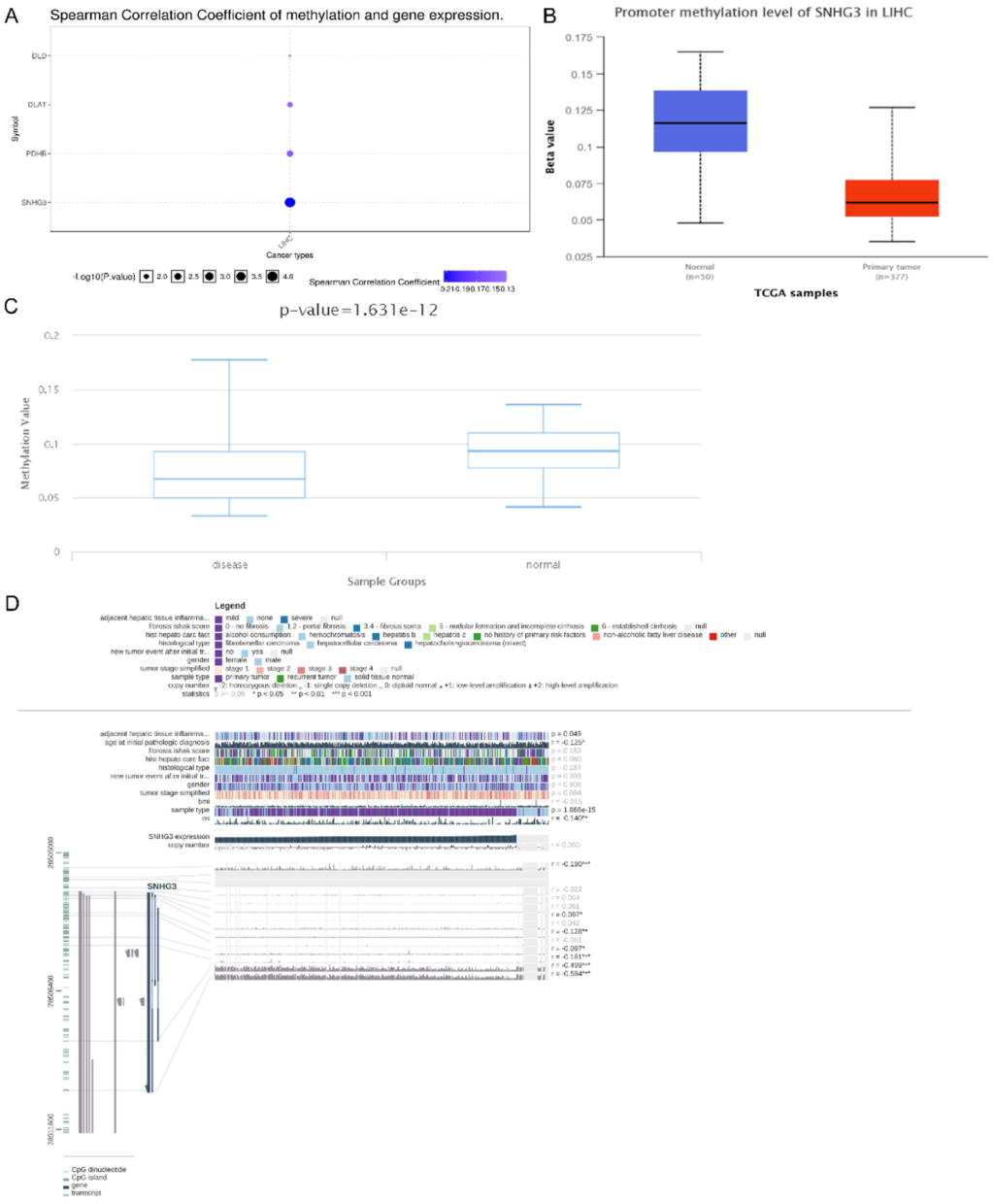

Figure 7. Methylation Analysis of SNHG3 in HCC. (A) Spearman correlation analysis of methylation and expression of SNHG3. (B) Methylation was evaluated using UALCAN. (C) Methylation was assessed using DiseaseMeth version 2.0. (D) Methylation site of SNHG3 DNA sequence association with gene expression was visualized using MEXPRESS. The expression of SNHG3 is illustrated by the blue line in the center of the plot. Pearson's correlation coefficients and *p* values for methylation sites and query gene expression are shown on the right side.

liver even the occurrence of liver cancer.[37] Ye et al. uncovered that oxalate and glycolate remarkably upregulated in recurrent HCC patients after surgery.[38] Mukha et al. found the crucial role of glycine cleavage system in maintaining mitochondrial protein lipoylation to support HCC growth.[39] Cellular response to chemical stress, including inflammatory response, oxidative stress, and extensive DNA damage, was recognized as driving factors of HCC.[40] A previous review explored the mechanisms of coagulation and fibrinolytic factors in the regulation of cancer growth.[41]

Hence, all of the above processes were linked to the initiation and progression of HCC, which suggested that cuproptosis-related genes were involved in the development of HCC. Additionally, protein−protein interaction analysis uncovered that these genes were tightly bound and the MOCDE algorithm identified two key clusters. In fact, the liver is the main organ of copper metabolism, and some evidence revealed that aberrant copper accumulation could increase the incidence of HCC. Therefore, we conjectured that cuproptosis was closely associated with the occurrence of HCC.

To identify the cuproptosis-related genes that play a crucial role in HCC carcinogenesis, we performed differential expression and survival analysis for MOCDE1 genes in the TCGA cohort. Two mRNAs (DLAT, PDHA1) were identified, which both upregulated in HCC and led to poor prognosis of HCC patients. It has been generally accepted that ncRNAs, including miRNAs, lncRNAs, and circRNAs, participated in gene expression modulation by competing with each other via the ceRNA mechanism.[42−45] Recent studies have also experimentally verified that lncRNAs could

https://doi.org/10.1021/acsomega.3c06018
ACS Omega 2023, 8, 38690−38703

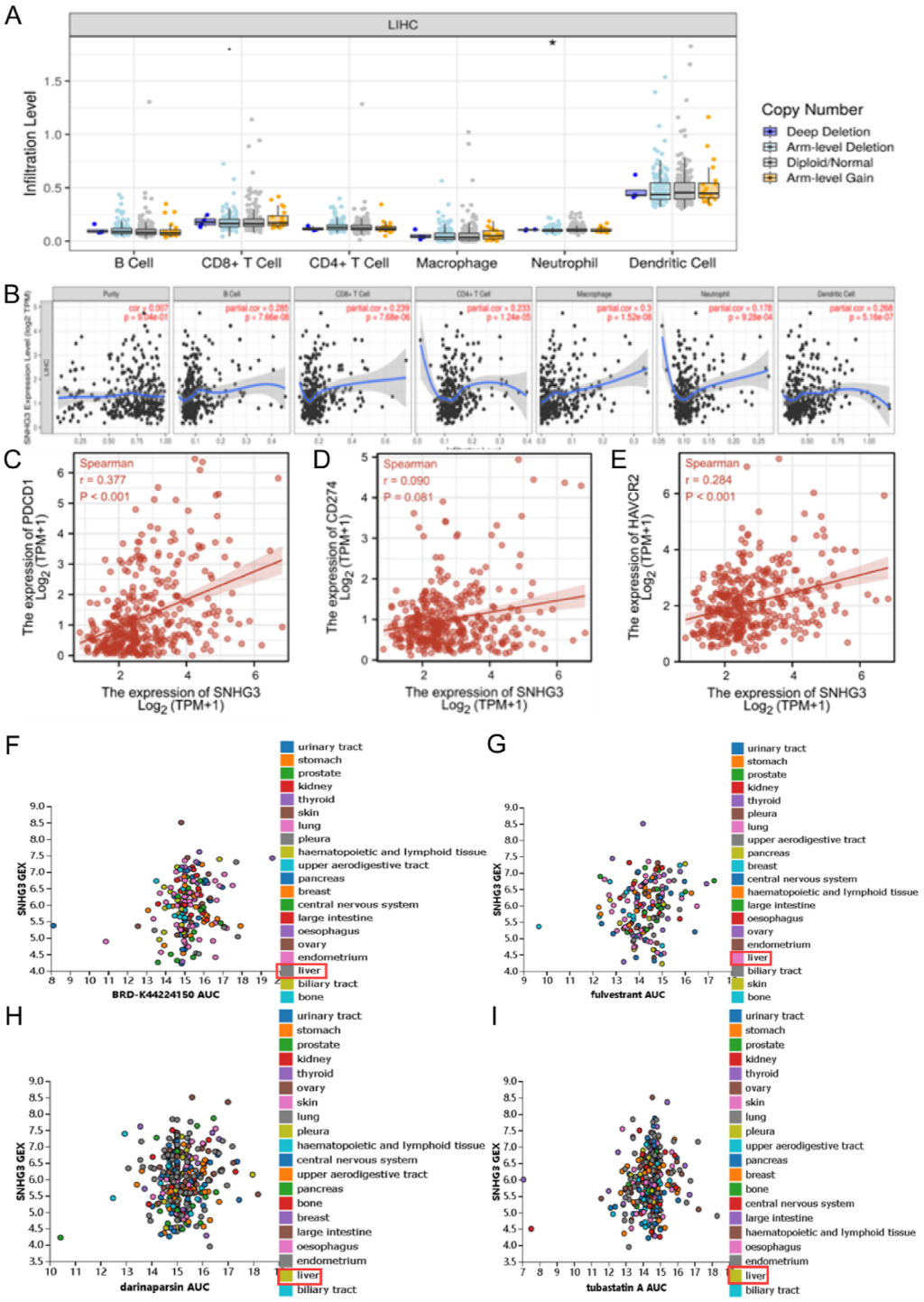

Figure 8. Immune infiltration and drug sensitivity analysis of SNHG3 in HCC. (A) Association between SNHG3 gene copy number and immune cell infiltration levels in HCC cohorts. (B) Correlation between SNHG3 expression and immune infiltration levels in HCC. (C–E) Association between SNHG3 expression and PDCD1 (C), CD274 (D), and HAVCR2 (E) expression in HCC patients, respectively. (F–I) Correlation between SNHG3 expression and drug sensitivity of BRD-K44224150 (F), fulvestrant (G), darinaparsin (H), and tubastain A (I). $*p < 0.05$, $**p < 0.01$, $***p < 0.001$.

regulate gene expression through sponging shared miRNAs, thus involving HCC progression. For example, Wang et al. suggested that lncRNA MAGI2-AS3 positively regulated the expression of FOXO1 through the induction of miR-374a/b-5p, thus facilitating the proliferation, migration, and invasion of HCC cells and increasing the apoptosis of HCC cells.[46] However, the prognostic impact of ceRNA on HCC has not been fully elucidated, and few studies have identified cuproptosis-related ceRNA regulatory networks that affect survival in patients with HCC. Accordingly, we intended to construct a cuproptosis-related ceRNA network that could predict HCC prognosis and provide a potential target for HCC treatment.

To find upstream regulatory miRNAs of DLAT and PDHA1, we utilized two prediction programs, the miRDB and the Tarbase v8 database, and a total of 75 miRNAs were

https://doi.org/10.1021/acsomega.3c06018
ACS Omega 2023, 8, 38690−38703

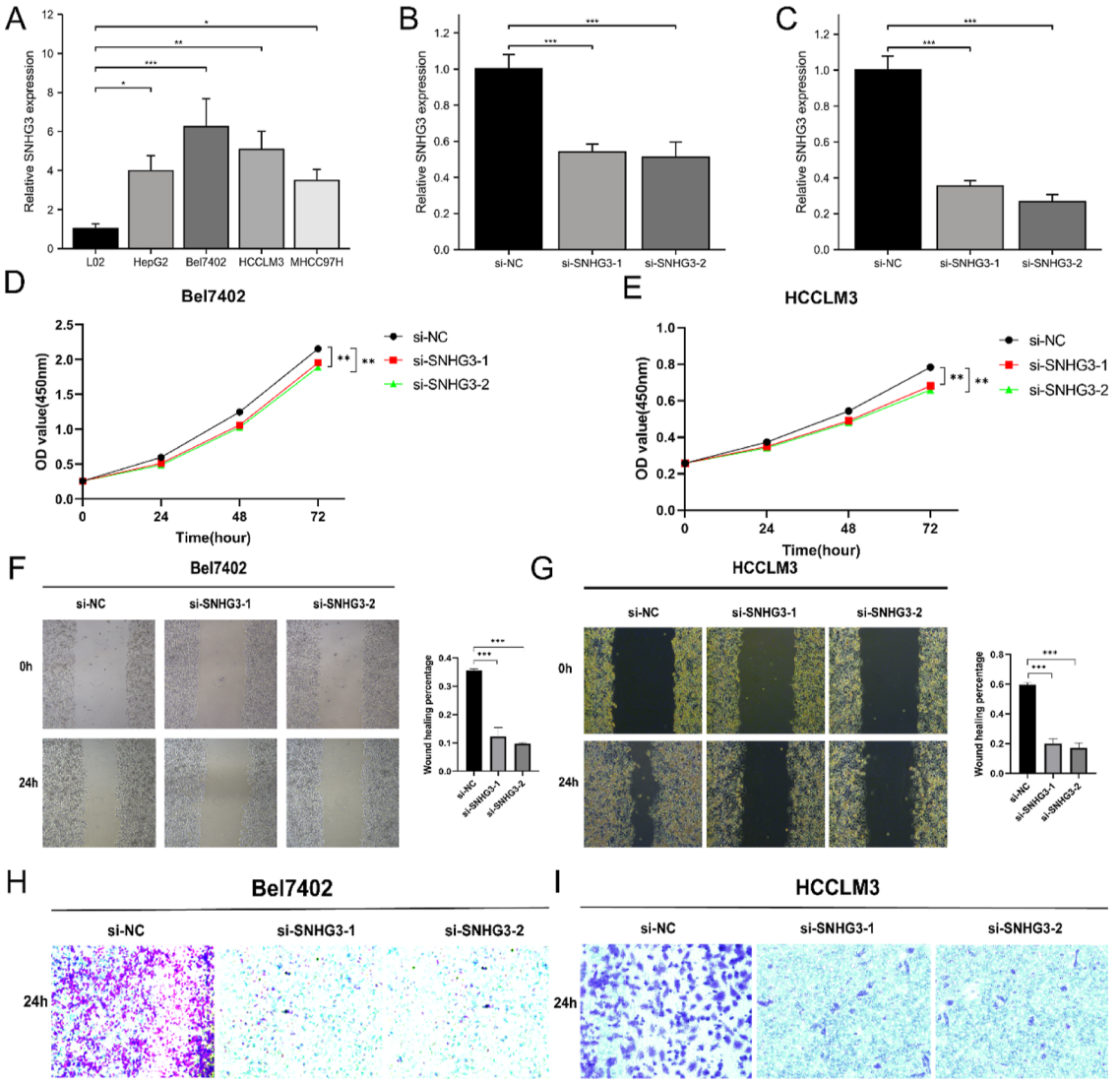

Figure 9. Relative SNHG3 expression by qRT-PCR and inhibition effects of SNHG3 knockdown on HCC in vitro. (A) SNHG3 expression in different liver cancer cell lines (HepG2, Bel7402, HCCLM3, and MHCC97H) compared with normal hepatocytes (L02). (B) Efficiency of SNHG3 knockdown in the Bel7402 cell line. (C) Efficiency of SNHG3 knockdown in the HCCLM3 cell line. (D,E) Proliferation ability of Bel7402 and HCCLM3 cells was significantly suppressed after SNHG3 silencing by CCK8 assay. (F,G) Migration ability of Bel7402 and HCCLM3 cells was significantly inhibited after SNHG3 silencing by wound healing assay. (H,I) Invasion capacity of Bel7402 and HCCLM3 cells was significantly weakened after SNHG3 silencing by transwell assay.

obtained. After performing survival analysis through the Oncolnc online database, miR-1306-5p was selected as the most potential upstream miRNA of PDHA1 in HCC. Next, upstream lncRNAs of miR-1306-5p/PDHA1 axis were also predicted by ENCORI and lncATLAS database, and two possible lncRNAs were found. We selected lncRNA SNHG3 after implementing subcellular localization analysis and demonstrated that SNHG3 was overexpressed in HCC, which was associated with poor OS of HCC patients. Taken together, the SNHG3/miR-1306-5p/PDHA1 axis was identified as a potential regulatory pathway in HCC.

Pyruvate dehydrogenase alpha 1 (PDHA1) is a rate-limiting enzyme that converts pyruvate into acetyl-CoA after entering the mitochondria, linking glycolysis aerobic oxidation to the TCA cycle and oxidative phosphorylation. Islam et al. proposed that phosphorylation of PDHA1 induced by insulin-regulated cell proliferation through the RhoA activation pathway in HepG2 cells.[47] Sun et al. uncovered that PDHA1 upregulation suppressed the Warburg effect and promoted cell apoptosis via mitochondria-mediated pathway in HCC.[48] miRNAs are a class of noncoding single-stranded RNA molecules encoded by endogenous genes that are about 22 nucleotides in length[49] and modulate gene expression by inhibiting the translation of mRNA or promoting their degradation.[50] Several studies have explored the role of miR-1306-5p in cancer progression. Gao et al. found that miR-1306-5p enhanced cell proliferation and suppressed cell apoptosis in acute myeloid leukemia.[51] Wang et al. uncovered that sponging miR-1306-5p could stimulate the malignant behaviors of melanoma cells.[52] MiR-1306-5p has also been reported to remarkably inhibits the malignant behavior of osteosarcoma cells.[53] Thus, miR-1306-5p may play multiple roles and even contradictory roles in regulating malignant behaviors via different mechanisms. However, there was no previous literature elucidating the role of miR-1306-5p in HCC progression. Our study found that miR-1306-5p expression

https://doi.org/10.1021/acsomega.3c06018
ACS Omega 2023, 8, 38690−38703

differed between the HCC tumor and normal tissues, and miR-1306-5p overexpression was correlated with a poor prognosis of HCC patients. lncRNA is a type of RNA molecule that participates in various intracellular processes.[54−56] Small nucleolar RNA host gene 3 (SNHG3) is a lncRNA located on chromosome 1p35.3 and aberrantly expressed in a variety of malignancies such as lung adenocarcinoma[57] and prostate cancer.[58] Zhang et al. discovered that SNHG3 promoted EMT and sorafenib resistance through miR-128/CD151 axis in HCC.[59] Wu et al. put forward that the SNHG3/miR-139-5p/BMI1 axis regulated the proliferation, migration, and invasion of HCC.[60] Thus, SNHG3 can play a role in HCC regulation via other ceRNA networks. Our newly proposed ceRNA network may regulate the malignant behavior of HCC through the same binding sites as other ceRNAs, forming large-scale regulatory networks and expanding the functional genetic information in the human genome. Moreover, the expression pattern of SNHG3/miR-1306-5p/PDHA1 conformed to the construction principles of the ceRNA network, which paved the way for in-depth research.

Next, we verified SNHG3 and PDHA1 abnormally high expression in HCC tissues using six independent GEO data sets as validation sets and conducted clinical correlation analysis of SNHG3 and PDHA1 in HCC patients. Both SNHG3 and PDHA1 were markedly related to the OS of HCC patients in univariate Cox analysis, and only SNHG3 was remarkably linked to the OS of HCC patients in multivariate Cox analysis. Therefore, SNHG3 is more likely to be an independent prognostic factor for HCC patients. To further exploit the potential clinical value of SNHG3 for the treatment of HCC, we carried out methylation, immune infiltration, and drug sensitivity analysis of SNHG3. It was proven that the methylation level of SNHG3 in normal samples was higher compared with HCC tumor samples, which suggested that methylation might be one of the reasons for the differential expression of SNHG3 in HCC and normal liver samples. According to the TIMER2.0 database, SNHG3 expression was tightly associated with infiltration abundance of some immune cells in the tumor microenvironment such as CD8+cells, macrophages, neutrophils, and dendritic cells. Moreover, we found that SNHG3 expression was positively linked to PDCD1 and HAVCR2 expression. In addition, we predicted half of the concentration of drugs that can kill cancer cells (IC50) based on the expression matrix of cancer cell lines in the CTRP database and drug treatment information. We found that SNHG3 expression was positively correlated with the drug sensitivity of BRD-K44224150, fulvestrant, darinaparsin, and tubastain A, which may become an effective strategy for the treatment and prognosis improvement of HCC.

Finally, our work found that SNHG3 expression detected by qRT-PCR was upregulated in liver cancer cell lines. In addition, we performed in vitro experiments and revealed that SNHG3 could significantly promote HCC proliferation, migration, and invasion. Based on the above analysis, we knew that SNHG3 upregulated PDHA1 via sponging miR-1306-5p and finally played a role in the HCC progression through PDHA1 overexpression. Given that PDHA1 was an indispensable component of pyruvate dehydrogenase (PDH) complex and participated in the TCA cycle, we speculated that SNHG3 upregulation competitively binding with miR-1306-5p thus unblocking its inhibition toward PDHA1 expression and PDHA1 overexpression could promote the process of TCA cycle and produced more energy which could be used for the proliferation, migration, and invasion of HCC.

Our study also has some defects. First, although we validated the robustness of the prognostic effect of screened cuproptosis gene-related ceRNA network in TCGA and GEO cohort, this study was only a retrospective study and further prospective studies with a sufficiently large sample scale are required to corroborate each other. Second, some samples in the TCGA and GEO cohorts lack clinical information, and no additional subgroups were analyzed because of data content limitations.

In conclusion, we constructed and validated a cuproptosis-related ceRNA regulatory axis for HCC patients, which could act as a prognostic indicator for clinical outcome and therapeutic response, bringing new insights into the molecular mechanism of HCC formation and progression.

■ ASSOCIATED CONTENT

Data Availability Statement

The original contributions presented in the study are included in the article/Supporting Information. Further inquiries can be directed to the corresponding author. Publicly available data sets were analyzed in this study. This data can be found here: https://portal.gdc.cancer.gov/, and http://www.ncbi.nlm.nih.gov/geo/.

Supporting Information

The Supporting Information is available free of charge at https://pubs.acs.org/doi/10.1021/acsomega.3c06018.

Baseline characteristics of the patients in TCGA cohort; cuproptosis-related genes and their functions; and summary of six GEO data sets involving HCC patients (PDF)

■ AUTHOR INFORMATION

Corresponding Author

Shibo Li − *Department of Infectious Disease, Zhoushan Hospital, Wenzhou Medical University, Zhoushan City 316021, China*; Email: lsb0398@126.com

Authors

Yong Pan − *Department of Infectious Disease, Zhoushan Hospital, Wenzhou Medical University, Zhoushan City 316021, China*; orcid.org/0009-0001-0837-9233

Yiru Zhang − *Department of Infectious Disease, Zhoushan Hospital, Wenzhou Medical University, Zhoushan City 316021, China; State Key Laboratory for the Diagnosis and Treatment of Infectious Diseases, The First Affiliated Hospital, Zhejiang University School of Medicine, Hangzhou City 310003, China*

Xiaodan Hu − *Department of Infectious Disease, Zhoushan Hospital, Wenzhou Medical University, Zhoushan City 316021, China*

Complete contact information is available at: https://pubs.acs.org/10.1021/acsomega.3c06018

Author Contributions

Y.P. and Y.Z. initiated the study and organized it; Y.P. and X.H. designed and carried out bioinformatics analyses, statistical analyses, drew figures, and drafted the manuscript; and S.L. contributed to the review and editing. All authors have read and agreed to the published version of the manuscript.

https://doi.org/10.1021/acsomega.3c06018
ACS Omega 2023, 8, 38690−38703

Funding

This work was supported by Zhejiang Province Major Science and Technology Project for Medicine and Health, grant number WKJ-ZJ-2329; General Scientific Research Project of Zhejiang Provincial Education Department, grant number Y202250086.

Notes

The authors declare no competing financial interest.

■ ACKNOWLEDGMENTS

We thank the investigators and patients in the TCGA and GEO for providing data. And we also appreciate that Dr. Haijie Ma gives us normal hepatocytes and liver cancer cells.

■ REFERENCES

(1) Sung, H.; Ferlay, J.; Siegel, R. L.; Laversanne, M.; Soerjomataram, I.; Jemal, A.; Bray, F. Global Cancer Statistics 2020: GLOBOCAN Estimates of Incidence and Mortality Worldwide for 36 Cancers in 185 Countries. *Ca-Cancer J. Clin.* **2021**, *71* (3), 209−249.

(2) Mehta, N. Hepatocellular carcinoma-how to determine therapeutic options. *Hepatol. Commun.* **2020**, *4* (3), 342−354.

(3) Wang, J. H.; Zhong, X. P.; Zhang, Y. F.; Wu, X. L.; Li, S. H.; Jian, P. E.; Ling, Y. H.; Shi, M.; Chen, M. S.; Wei, W.; Guo, R. P. Cezanne predicts progression and adjuvant tace response in hepatocellular carcinoma. *Cell Death Dis.* **2017**, *8* (9), No. e3043.

(4) Yang, J. D.; Hainaut, P.; Gores, G. J.; Amadou, A.; Plymoth, A.; Roberts, L. R. A global view of hepatocellular carcinoma: Trends, risk, prevention and management. *Nat. Rev. Gastroenterol. Hepatol.* **2019**, *16* (10), 589−604.

(5) Johnson, P.; Zhou, Q.; Dao, D. Y.; Lo, Y. M. D. Circulating biomarkers in the diagnosis and management of hepatocellular carcinoma. *Nat. Rev. Gastroenterol. Hepatol.* **2022**, *19* (10), 670−681.

(6) Panda, D. Role of surveillance in prevention of hepatocellular carcinoma. *J. Clin. Exp. Hepatol.* **2014**, *4* (Suppl 3), S43−S49.

(7) Pinter, M.; Jain, R. K.; Duda, D. G. The Current Landscape of Immune Checkpoint Blockade in Hepatocellular Carcinoma: A Review. *JAMA Oncol.* **2021**, *7* (1), 113−123.

(8) Torre, L. A.; Bray, F.; Siegel, R. L.; Ferlay, J.; Lortet-Tieulent, J.; Jemal, A. Global cancer statistics,2012. *Ca-Cancer J. Clin.* **2015**, *65* (2), 87−108.

(9) Lim, D. H.; Casadei-Gardini, A.; Lee, M. A.; Lonardi, S.; Kim, J. W.; Masi, G.; Chon, H. J.; Rimini, M.; Kim, I.; Cheon, J.; et al. Prognostic implication of serum AFP in patients with hepatocellular carcinoma treated with regorafenib. *Future Oncol.* **2022**, *18* (27), 3021−3030.

(10) Malaguarnera, G.; Giordano, M.; Paladina, I.; Berretta, M.; Cappellani, A.; Malaguarnera, M. Serum markers of hepatocellular carcinoma. *Dig. Dis. Sci.* **2010**, *55*, 2744−2755.

(11) Vitale, A.; Farinati, F.; Finotti, M.; Di Renzo, C.; Brancaccio, G.; Piscaglia, F.; Cabibbo, G.; Caturelli, E.; Missale, G.; Marra, F.; et al. Overview of Prognostic Systems for Hepatocellular Carcinoma and ITA.LI.CA External Validation of MESH and CNLC Classifications. *Cancers* **2021**, *13* (7), 1673.

(12) Salmena, L.; Poliseno, L.; Tay, Y.; Kats, L.; Pandolfi, P. P. A ceRNA hypothesis: the Rosetta Stone of a hidden RNA language? *Cell* **2011**, *146* (3), 353−358.

(13) Tay, Y.; Rinn, J.; Pandolfi, P. The multilayered complexity of ceRNA crosstalk and competition. *Nature* **2014**, *505* (7483), 344−352.

(14) Statello, L.; Guo, C. J.; Chen, L. L.; Huarte, M. Gene regulation by long non-coding RNAs and its biological functions. *Nat. Rev. Mol. Cell Biol.* **2021**, *22* (2), 96−118.

(15) Li, G.; Wang, Z.; Chen, D.; Yin, J.; Mo, Z.; Sun, B.; Yang, T.; Zhang, X.; Zhai, Z.; Li, Y.; et al. Comprehensive analysis of a TPX2-related TRHDE-AS1/PKIA ceRNA network involving prognostic signatures in Hepatitis B virus-infected hepatocellular carcinoma. *Front. Cell. Infect. Microbiol.* **2022**, *12*, 1025900.

(16) Hao, F.; Wang, N.; Gui, H.; Zhang, Y.; Wu, Z.; Wang, J. Pseudogene UBE2MP1 derived transcript enhances in vitro cell proliferation and apoptosis resistance of hepatocellular carcinoma cells through miR-145-5p/RGS3 axis. *Aging* **2022**, *14* (19), 7906−7925.

(17) Kerr, J.; Wyllie, A.; Currie, A. Apoptosis: A Basic Biological Phenomenon with Wideranging Implications in Tissue Kinetics. *Br. J. Cancer* **1972**, *26* (4), 239−257.

(18) Degterev, A.; Huang, Z.; Boyce, M.; Li, Y.; Jagtap, P.; Mizushima, N.; Cuny, G. D.; Mitchison, T. J.; Moskowitz, M. A.; Yuan, J.; et al. Chemical inhibitor of nonapoptotic cell death with therapeutic potential for ischemic brain injury. *Nat. Chem. Biol.* **2005**, *1* (2), 112−119.

(19) Cookson, B.; Brennan, M. Pro-inflammatory programmed cell death. *Trends Microbiol.* **2001**, *9* (3), 113−114.

(20) Dixon, S. J.; Lemberg, K. M.; Lamprecht, M. R.; Skouta, R.; Zaitsev, E. M.; Gleason, C. E.; Patel, D. N.; Bauer, A. J.; Cantley, A. M.; Yang, W. S.; et al. Ferroptosis:An Iron-Dependent Form of Nonapoptotic Cell Death. *Cell* **2012**, *149* (5), 1060−1072.

(21) Tsvetkov, P.; Coy, S.; Petrova, B.; Dreishpoon, M.; Verma, A.; Abdusamad, M.; Rossen, J.; Joesch-Cohen, L.; Humeidi, R.; Spangler, R. D.; et al. Copper Induces Cell Death by Targeting Lipoylated TCA Cycle Proteins. *Science* **2022**, *375* (6586), 1254−1261.

(22) Lelièvre, P.; Sancey, L.; Coll, J. L.; Deniaud, A.; Busser, B. The Multifaceted Roles of Copper in Cancer: A Trace Metal Element with Dysregulated Metabolism, but Also a Target or a Bullet for Therapy. *Cancers* **2020**, *12* (12), 3594.

(23) Ge, E. J.; Bush, A. I.; Casini, A.; Cobine, P. A.; Cross, J. R.; DeNicola, G. M.; Dou, Q. P.; Franz, K. J.; Gohil, V. M.; Gupta, S.; et al. Connecting copper and cancer: from transition metal signalling to metalloplasia. *Nat. Rev. Cancer* **2022**, *22* (2), 102−113.

(24) Jiang, Y.; Huo, Z.; Qi, X.; Zuo, T.; Wu, Z. Copper-induced tumor cell death mechanisms and antitumor theragnostic applications of copper complexes. *Nanomedicine* **2022**, *17* (5), 303−324.

(25) Jin, C.; Li, Y.; Su, Y.; Guo, Z.; Wang, X.; Wang, S.; Zhang, F.; Zhang, Z.; Shao, J.; Zheng, S. Novel copper complex CTB regulates methionine cycle induced TERT hypomethylation to promote HCC cells senescence via mitochondrial SLC25A26. *Cell Death Dis.* **2020**, *11* (10), 844.

(26) Yang, M.; Wu, X.; Li, L.; Li, S.; Li, N.; Mao, M.; Pan, S.; Du, R.; Wang, X.; Chen, M.; et al. COMMD10 inhibits tumor progression and induces apoptosis by blocking NF-κB signal and values up BCLC staging in predicting overall survival in hepatocellular carcinoma. *Clin. Transl. Med.* **2021**, *11* (5), No. e403.

(27) Yang, M.; Wu, X.; Hu, J.; Wang, Y.; Wang, Y.; Zhang, L.; Huang, W.; Wang, X.; Li, N.; Liao, L.; et al. COMMD10 inhibits HIF1α/CP loop to enhance ferroptosis and radiosensitivity by disrupting Cu-Fe balance in hepatocellular carcinoma. *J. Hepatol.* **2022**, *76* (5), 1138−1150.

(28) Kim, B. E.; Nevitt, T.; Thiele, D. J. Mechanisms for copper acquisition, distribution and regulation. *Nat. Chem. Biol.* **2008**, *4* (3), 176−185.

(29) Zhou, Y.; Zhou, B.; Pache, L.; Chang, M.; Khodabakhshi, A. H.; Tanaseichuk, O.; Benner, C.; Chanda, S. K. Metascape provides a biologist-oriented resource for the analysis of systems-level datasets. *Nat. Commun.* **2019**, *10* (1), 1523.

(30) Bader, G. D.; Hogue, C. W. An automated method for finding molecular complexes in large protein interaction networks. *BMC Bioinf.* **2003**, *4*, 2.

(31) Shannon, P.; Markiel, A.; Ozier, O.; Baliga, N. S.; Wang, J. T.; Ramage, D.; Amin, N.; Schwikowski, B.; Ideker, T. Cytoscape: a software environment for integrated models of biomolecular interaction networks. *Genome Res.* **2003**, *13* (11), 2498−2504.

(32) Mas-Ponte, D.; Carlevaro-Fita, J.; Palumbo, E.; Hermoso Pulido, T.; Guigo, R.; Johnson, R. LncATLAS database for subcellular localization of long noncoding RNAs. *RNA* **2017**, *23* (7), 1080−1087.

https://doi.org/10.1021/acsomega.3c06018
ACS Omega 2023, 8, 38690−38703

(33) Liu, C. J.; Hu, F. F.; Xia, M. X.; Han, L.; Zhang, Q.; Guo, A. Y. GSCALite: a web server for gene set cancer analysis. *Bioinformatics* **2018**, *34* (21), 3771−3772.
(34) Li, T.; Fan, J.; Wang, B.; Traugh, N.; Chen, Q.; Liu, J. S.; Li, B.; Liu, X. S. TIMER: A Web Server for Comprehensive Analysis of Tumor-Infiltrating Immune Cells. *Cancer Res.* **2017**, *77* (21), e108−e110.
(35) Sturm, G.; Finotello, F.; Petitprez, F.; Zhang, J. D.; Baumbach, J.; Fridman, W. H.; List, M.; Aneichyk, T. Comprehensive evaluation of transcriptome-based cell-type quantification methods for immuno-oncology. *Bioinformatics* **2019**, *35* (14), i436−i445.
(36) He, X.; Xu, C. Immune checkpoint signaling and cancer immunotherapy. *Cell Res.* **2020**, *30* (8), 660−669.
(37) Wu, Z.; Lv, G.; Xing, F.; Xiang, W.; Ma, Y.; Feng, Q.; Yang, W.; Wang, H. Copper in hepatocellular carcinoma: A double-edged sword with therapeutic potentials. *Cancer Lett.* **2023**, *571*, 216348.
(38) Ye, G.; Zhu, B.; Yao, Z.; Yin, P.; Lu, X.; Kong, H.; Fan, F.; Jiao, B.; Xu, G. Analysis of urinary metabolic signatures of early hepatocellular carcinoma recurrence after surgical removal using gas chromatography-mass spectrometry. *J. Proteome Res.* **2012**, *11* (8), 4361−4372.
(39) Mukha, D.; Fokra, M.; Feldman, A.; Sarvin, B.; Sarvin, N.; Nevo-Dinur, K.; Besser, E.; Hallo, E.; Aizenshtein, E.; Schug, Z. T.; Shlomi, T. Glycine decarboxylase maintains mitochondrial protein lipoylation to support tumor growth. *Cell Metab.* **2022**, *34* (5), 775−782.e9.
(40) Si, Z.; Yang, G.; Wang, X.; Yu, Z.; Pang, Q.; Zhang, S.; Qian, L.; Ruan, Y.; Huang, J.; Yu, L. An unconventional cancer-promoting function of methamphetamine in hepatocellular carcinoma. *Life Sci. Alliance* **2023**, *6* (3), No. e202201660.
(41) Li, X.; Gu, B.; Wang, B.; Feng, Z.; Ma, Y.; Li, H.; Lucas, A.; Chen, H. Intrahepatic metastases may be specific to hepatocellular carcinoma due to the coagulation and fibrinolytic systems (Review). *Oncol. Rep.* **2020**, *44* (6), 2345−2352.
(42) He, Q.; Hao, Q.; Wu, Y.; Vadgama, J. V.; Jiang, Y. CircRAD54L2 promotes triple-negative breast cancer progression by regulating the miR-888 family/PDK1 axis. *Life Sci.* **2023**, *312*, 121128.
(43) Xu, Y.; Luan, G.; Li, Z.; Liu, Z.; Qin, G.; Chu, Y. Tumour-derived exosomal lncRNA SNHG16 induces telocytes to promote metastasis of hepatocellular carcinoma via the miR-942-3p/MMP9 axis. *Cell Oncol.* **2023**, *46* (2), 251−264.
(44) Razavi, Z. S.; Tajiknia, V.; Majidi, S.; Ghandali, M.; Mirzaei, H. R.; Rahimian, N.; Hamblin, M. R.; Mirzaei, H. Gynecologic cancers and non-coding RNAs: Epigenetic regulators with emerging roles. *Crit. Rev. Oncol. Hematol.* **2021**, *157*, 103192.
(45) Fabrizio, F.; Sparaneo, A.; Muscarella, L. NRF2 Regulation by Noncoding RNAs in Cancers: The Present Knowledge and the Way Forward. *Cancers* **2020**, *12* (12), 3621.
(46) Wang, C.; Su, K.; Lin, H.; Cen, B.; Zheng, S.; Xu, X. Identification and Verification of a Novel MAGI2-AS3/miRNA-374-5p/FOXO1 Network Associated with HBV-Related HCC. *Cells* **2022**, *11* (21), 3466.
(47) Islam, R.; Kim, J. G.; Park, Y.; Cho, J. Y.; Cap, K. C.; Kho, A. R.; Chung, W. S.; Suh, S. W.; Park, J. B. Insulin induces phosphorylation of pyruvate dehydrogenase through RhoA activation pathway in HepG2 cells. *FASEB J.* **2019**, *33* (2), 2072−2083.
(48) Sun, J.; Li, J.; Guo, Z.; Sun, L.; Juan, C.; Zhou, Y.; Gu, H.; Yu, Y.; Hu, Q.; Kan, Q.; Yu, Z. Overexpression of Pyruvate Dehydrogenase E1α Subunit Inhibits Warburg Effect and Induces Cell Apoptosis Through Mitochondria-Mediated Pathway in Hepatocellular Carcinoma. *Oncol. Res.* **2019**, *27* (4), 407−414.
(49) Tiwari, A.; Mukherjee, B.; Dixit, M. MicroRNA Key to Angiogenesis Regulation: MiRNA Biology and Therapy. *Curr. Cancer Drug Targets* **2018**, *18* (3), 266−277.
(50) Correia de Sousa, M.; Gjorgjieva, M.; Dolicka, D.; Sobolewski, C.; Foti, M. Deciphering miRNAs' Action through miRNA Editing. *Int. J. Mol. Sci.* **2019**, *20* (24), 6249.
(51) Gao, X.; Fan, S.; Zhang, X. MiR-1306−5p promotes cell proliferation and inhibits cell apoptosis in acute myeloid leukemia by downregulating PHF6 expression. *Leuk. Res.* **2022**, *120*, 106906.
(52) Wang, K.; Li, M.; Duan, H.; Fan, M.; Xu, C.; Yu, F. SLCO4A1-AS1 triggers the malignant behaviours of melanoma cells via sponging miR-1306−5p to enhance PCGF2. *Exp. Dermatol.* **2022**, *31* (8), 1220−1233.
(53) Dang, Y.; Zhou, Y.; Ou, X.; Wang, Q.; Wei, D.; Xie, F. lncRNA AC007207.2 Promotes Malignant Properties of Osteosarcoma via the miR-1306−5p/SIRT7 Axis. *Cancer Manage. Res.* **2021**, *13*, 7277−7288.
(54) Quinn, J. J.; Chang, H. Y. Unique features of long non-coding RNA biogenesis and function. *Nat. Rev. Genet.* **2016**, *17* (1), 47−62.
(55) Batista, P.; Chang, H. Long noncoding RNAs: cellular address codes in development and disease. *Cell* **2013**, *152* (6), 1298−1307.
(56) Atianand, M.; Caffrey, D.; Fitzgerald, K. Immunobiology of Long Noncoding RNAs. *Annu. Rev. Immunol.* **2017**, *35*, 177−198.
(57) Liu, L.; Ni, J.; He, X. Upregulation of the Long Noncoding RNA SNHG3 Promotes Lung Adenocarcinoma Proliferation. *Dis. Markers* **2018**, *2018*, 1−12.
(58) Wang, X.; Song, Y.; Shi, Y.; Yang, D.; Li, J.; Yin, B. SNHG3 could promote prostate cancer progression through reducing methionine dependence of PCa cells. *Cell. Mol. Biol. Lett.* **2022**, *27* (1), 13.
(59) Zhang, P. F.; Wang, F.; Wu, J.; Wu, Y.; Huang, W.; Liu, D.; Huang, X. Y.; Zhang, X. M.; Ke, A. W. LncRNA SNHG3 induces EMT and sorafenib resistance by modulating the miR-128/CD151 pathway in hepatocellular carcinoma. *J. Cell. Physiol.* **2019**, *234* (3), 2788−2794.
(60) Wu, J.; Liu, L.; Jin, H.; Li, Q.; Wang, S.; Peng, B. <p>LncSNHG3/miR-139-5p/BMI1 axis regulates proliferation, migration, and invasion in hepatocellular carcinoma</p> *OncoTargets Ther.* **2019**, *12*, 6623−6638.

https://doi.org/10.1021/acsomega.3c06018
ACS Omega 2023, 8, 38690−38703